Soil Biology and Biochemistry 202 (2025) 109691

Contents lists available at ScienceDirect

Soil Biology and Biochemistry

journal homepage: www.elsevier.com/locate/soilbio

Coupling energy balance and carbon flux during cellulose degradation in arable soils

Johannes Wirsching [a,1], Martin-Georg Endress [b,1], Eliana Di Lodovico [c], Sergey Blagodatsky [b,d], Christian Fricke [c,f], Marcel Lorenz [e], Sven Marhan [a], Ellen Kandeler [a], Christian Poll [a,*]

[a] Institute of Soil Science and Land Evaluation, Soil Biology Department, University of Hohenheim, Germany
[b] Institute of Zoology, Faculty of Mathematics and Natural Sciences, University of Cologne, Germany
[c] Faculty of Natural and Environmental Sciences, University of Kaiserslautern-Landau, Germany
[d] Campus Alpin, Institute of Meteorology and Climate Research, Department of Atmospheric Environmental Research (IMK-IFU), Karlsruhe Institute of Technology (KIT), Germany
[e] Department of Soil Science, University of Trier, Helmholtz Centre for Environmental Research, Leipzig, Germany
[f] Berufsakademie Sachsen–Staatliche Studienakademie Riesa, University of Cooperative Education, Germany

ARTICLE INFO

Keywords:
Energy use efficiency (EUE)
Calorimetric ratio (CR)
Carbon use efficiency (CUE)
^{13}C-Labeled cellulose
Fertilized and unfertilized arable soils

ABSTRACT

Microbial carbon use efficiency (CUE) is an important metric for understanding the balance between anabolic and catabolic metabolism, while energy use efficiency (EUE) provides insight into microbial energy requirements. They are linked by the ratio between released heat and respiration (calorespirometric ratio, CR), which can be used to describe the efficiency of microbial growth. In this study, microbial C and energy use during the degradation of ^{13}C-labeled cellulose in eight different soils was investigated experimentally and simulated using a process-based model. Our results show close agreement between the cumulative C and energy balances during the incubations, with a total C and energy release equal to 30–50% of the amount added as cellulose. Both energy and C fluxes indicated that a positive priming effect of soil organic matter (SOM) increased the release of heat and CO_2 by 10–32% relative to the added substrate. The CR-CUE relationship indicated that growth on cellulose was energy limited during the early but not the later stages of the incubation, especially in soils with high SOM content. We partly observed systematic differences between estimates for CUE based either on the ^{13}C label or on the calorespirometric ratio. Both approaches were constrained by technical and methodological limitations and agreed best during the phase of microbial growth in the SOM-rich soils, with CUE values between 0.4 and 0.75 indicating efficient aerobic growth. During early stages or after transition to a maintenance phase, both estimates were less meaningful for cellulose degradation, a substrate with a lower turnover rate than glucose. Still, the coupled heat and mass balances during cellulose degradation in combination with process-based modeling provided additional information on growth yields as well as the contribution of SOM priming to microbial growth compared to considering mass balances alone.

1. Introduction

Microorganisms utilize soil organic matter (SOM) for catabolic and anabolic processes (Chakrawal et al., 2020). This C allocation or the ratio of C used for biosynthesis to C consumed is commonly referred to as carbon use efficiency (CUE; (Geyer et al., 2019)), from which we can deduce how much C is either emitted from the soil as CO_2 or retained and eventually stabilized in the SOM (Chakrawal et al., 2020). Studies have highlighted the importance of substrate availability, nutrient composition, environmental conditions, and microbial community composition to explain the variability in CUE (Manzoni et al., 2012; Qiao et al., 2019; Domeignoz-Horta et al., 2020). What is missing are

This article is part of a special issue entitled: Soil C and energy fluxes published in Soil Biology and Biochemistry.

* Corresponding author.
E-mail address: christian.poll@uni-hohenheim.de (C. Poll).

[1] Authors contributed equally.

https://doi.org/10.1016/j.soilbio.2024.109691
Received 28 June 2024; Received in revised form 20 November 2024; Accepted 9 December 2024
Available online 11 December 2024

studies that take into account that biosynthesis is a purely non-equilibrium process that depends not only on carbon alone but also on the energy that can be provided by catabolism (Kästner et al., 2024). This perspective emphasizes the quantification of energy fluxes alongside traditional carbon-centered analyses. Currently, there are a growing number of model-based descriptions, such as those published by Chakrawal et al. (2020), in which the potential application of coupled mass and energy balance models for glucose can be used to create a generalized understanding of metabolic pathways during substrate utilization and implement physiological constraints in C-cycle models (Calabrese et al., 2021; Endress et al., 2024a). However, there is a lack of experimental data to support this theoretical notion, also with regard to more complex molecules that better reflect the natural composition of fresh litter in the soil, e.g. cellulose, while revealing possible technical limitations in determining and combining energy and mass fluxes.

The measurement of heat production via calorimetry opens up a non-destructive, label-free method in soil science that provide useful thermodynamic, kinetic and stochiometric quantities (Yang et al., 2024). One of these is the calorespirometric ratio (CR), i.e. the quotient of the specific heat (Q_t; kJ g^{-1}) and the CO_2 release (R_{CO_2}; mol CO_2–C g^{-1}). This ratio contains valuable information about the soil microbial metabolism, because it reflects the fact that a certain fraction of energy contained in the substrate is released as heat during catabolic oxidation of substrate-C to CO_2, while the remainder is used for reducing C during biosynthesis. Hence, it links heat and CO_2 production during substrate consumption to the efficiency with which microorganisms synthesize new biomass from the substrate. Hansen et al. (2004) developed a widely used quantitative model linking the CR to CUE which allows estimating the CUE of microbial growth from the simultaneous measurement of heat and CO_2 production. This model simplifies soil processes by focusing on aerobic metabolic processes and a single substrate and neglecting any interactions involving minerals or SOM (Yang et al., 2024). Building on these findings, Chakrawal et al. (2020) expanded the model to include both SOM utilization as well as anaerobic processes such as ethanol and lactic acid fermentation. This extension enabled a more comprehensive and nuanced understanding of CR-CUE relationships. In particular, the authors showed how the CR-CUE relationship for a simple microbial growth reaction differs depending on the energy content of the substrate: if a substrate that is more oxidized than microbial biomass is consumed, the CR values decrease with increasing CUE and are limited to values below the combustion enthalpy (=energy content) of the biomass, whereas more reduced substrates result in CR values that increase with increasing CUE and fall above this threshold. The former corresponds to energy limited growth with relatively more C than energy being released per unit substrate, while the latter corresponds to C-limited growth, with relatively more energy than C being released (Chakrawal et al., 2020). The CR-CUE relation in the complex soil environment can, however, be influenced by many other factors that may cause deviations from such simple predictions (Barros et al., 2016; Herrmann and Bölscher, 2015). For instance, technical limitations may result in alterations to the CR when attempting to carry out the combined measurement of heat and CO_2 in parallel experiments in separate vessels (Yang et al., 2024; Endress et al., 2024b). Other processes that consume C and energy such as the production of extracellular enzymes or the formation of biofilms (Bölscher et al., 2024), might also affect the CR-CUE relation through the anabolic use of C that is not directly linked to biomass production. Similarly, extracellular enzymes can release heat during hydrolysis and depolymerization of complex substrates, which could elevate measured CR values. The additional use of SOM after substrate addition can contribute to microbial growth and, hence, to heat production that is not directly linked to the added substrate (Arcand et al., 2017). The intensity of priming depends, among other factors, on the competition for energy and nutrients between microbial groups using the fresh added substrate and other groups using SOM (Fontaine et al., 2003). The degree to which SOM priming affects the CR-CUE relation depends, therefore, also on the amount and energy content of the SOM.

The different substrate preference and growth strategies control not only the decomposition rate but also the course of CUE (De Graaff et al., 2010). According to Geyer et al. (2016), the beginning of substrate utilization is characterized by a population-level CUE, which is determined by species-specific metabolic and thermodynamic constraints and, over time, transforms into an ecosystem-level CUE reflecting the efficiency of microbial net biomass production (growth) per unit of ingested substrate, including recycling of microbial products (Geyer et al., 2016). An often-used method for estimating CUE is the use of ^{13}C-labeled substrates in conjunction with measuring the ^{13}C-flux into CO_2 and the microbial biomass. However, both methods (i.e. the quantitative model of Hansen et al. (2004) and ^{13}C-labeled substrates) have their specific strengths and weaknesses and a simultaneous application of both may provide new insights into the C and energy use of soil microorganisms (Geyer et al., 2019). In addition, the CO_2 and heat release (including priming of SOM) can be related to the amount of C and energy initially added to the soil as substrate. Such a comparison accounts both for CO_2 and heat production from other sources as well as for any incomplete decomposition of the added substrate, and is referred to in this study as net carbon balance (CB_{net}) and net energy use efficiency (EUE_{net}, Fig. 1). Both might be considered as the storage efficiency of the soil system (Manzoni et al., 2018) and CB_{net} might be seen in a continuum following population CUE and ecosystem CUE. In this context, a CB_{net} and $EUE_{net} > 0$ indicate a net C and energy gain in the soil system after substrate addition, while negative values indicate net C and energy loss from the system. It is important to note, that EUE_{net} differs from (instantaneous) EUE, which is defined as the fraction of total substrate-derived energy required for anabolism (Klemm et al., 2005; Wang and Kuzyakov, 2023). EUE_{net} can, therefore, only be related to CB_{net} and both are not directly relatable to the CUE estimates derived from ^{13}C mass balance or CR, but instead broaden the concepts of CUE and EUE.

The research aim of this study was to investigate the C and energy use from added cellulose in either organically fertilized or unfertilized arable soils during a 64-days incubation. We used ^{13}C-labeled cellulose and isothermal calorimetry in combination with a process-based model to provide an in-depth analysis of microbial cellulose degradation. This approach was used to address the following objectives: 1) apply and evaluate the concepts of CB_{net}, EUE_{net}, CR and CUE to cellulose degradation and 2) determine if growth on cellulose is energy limited as

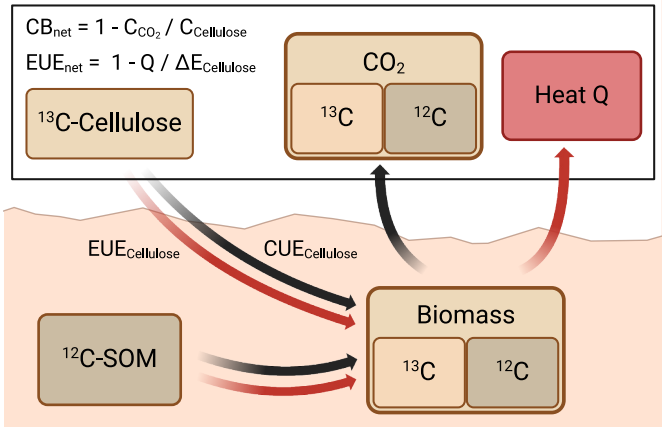

Fig. 1. Schematic of major C and energy flows in soil incubation experiments. Microorganisms consume ^{13}C-labeled substrate added to the soil to form new biomass, CO_2 and heat with a certain carbon and energy use efficiency ($CUE_{Cellulose}$ and $EUE_{Cellulose}$). Additionally, they also metabolize native (^{12}C-)SOM. The net storage or release of C (CB_{net}) and energy (EUE_{net}) in the soil thus depends on the balance between the total amount of C and energy initially added as substrate ($C_{Cellulose}$, $\Delta E_{Cellulose}$) on the one hand and the total amount of C and energy lost as CO_2 and heat over time (C_{CO_2}, Q) on the other hand.

predicted based on its energy content (Chakrawal et al., 2020). Furthermore, we want to 3) determine how priming of SOM and the fertilizer status affects CUEs, CB_{net} and EUE_{net}, and finally 4) evaluate technical difficulties in measuring and combining heat and CO_2 release in the CR.

2. Materials and methods

2.1. Soil origin and sampling

The soil samples originate from four long-term field experiments, each with an unfertilized (UF) and a fertilized (FYM) variant. The soils included in the study had different textures: a loamy sand called "Thyrow" (TH), a sandy loam called "Dikopshof" (DI), a loamy sand called "Reckenholz" (RE), and a silty loam called "QualiAgro" (QA). The soils cover a wide range of soil properties of arable soils, which allowed us to study the impact of background SOM and energy content on microbial cellulose utilization. Further details on the soil properties can be found in the published database (Lorenz et al., 2024a). Sampling was carried out randomly with a spade from the top 20 cm after harvest. Soil sampling took place in August for DI, in September for QA and RE and in October for TH, each in 2021. Thyrow (TH) is located at 52°16′N, 13°12′E in Brandenburg, Germany. The climate is characterized by an annual mean temperature of 9.2 °C and precipitation of 510 mm. The crop rotation, which has been implemented since 2005, consists of silage maize and winter rye. Since 1938, fertilizer has been applied exclusively with farmyard manure, which is applied at a rate of 20 t ha^{-1} (Ellmer and Baumecker, 2005; Kroschewski et al., 2023). The Dikopshof (DI) agricultural area is located at 50°81′N, 6°95′E in North Rhine-Westphalia, Germany. The area has an average annual temperature of 10.5 °C and a precipitation of 688 mm. Since 1953, the farm has been cultivated as part of a five-year crop rotation, with sugar beet, winter wheat, winter rye, Persian clover and potatoes being grown. Since 1904, farmyard manure has been applied at a rate of 60 t ha^{-1} (Ahrends et al., 2018). The Reckenholz (RE) site is an arable field at 47°43′ N, 8°52′ E near Zurich, Switzerland. Reckenholz has an annual mean temperature of 9.5 °C and a precipitation of 1050 mm. The 8-year crop rotation includes winter wheat, maize, potatoes, winter wheat, maize and spring barley. Since 1949, 5 t ha^{-1} of farm manure has been applied every second year (Cagnarini et al., 2021). QualiAgro (QA) soil samples were collected from a field situated at 48°87′ N, 1°95′ E in Île-de-France, with an average annual temperature of 10.8 °C and 644 mm of precipitation. The crop rotation includes barley, oats, barley and maize, with farmyard manure applied at a rate of 4 t ha^{-1} every two years since 2014 (Nest et al., 2016).

2.2. Experimental design

The soils were stored air-dry and pre-incubated for 10 days at a water content corresponding to 45–50% water holding capacity (Supplementary Table S2, Table S3) to restore and stabilize microbial activity. After pre-incubation, the soils were incubated with 97 at% ^{13}C-labeled cellulose derived from maize (*Zea mays*; IsoLife, Wageningen, Netherlands). The amount added corresponded to four times the C content of the microbial biomass in each soil (Table 1).

The cellulose was frozen at −80 °C and ground in a ball mill to a fine powder that allowed homogeneous mixing with the soil. Soils without cellulose addition served as controls. Soil equivalent to 3.78 g dry matter was incubated in 20 ml airtight calorimeter vials, which, together with aeration of the vials at three time points, ensured sufficient oxygen availability during the incubation. The experiment was run for 64 days in three replicates, with the assumption that a significant proportion would be utilized by that time. Additional sets of vials were sampled at 4, 8, 16 and 32 days to cover, together with the frequent respiration measurements, the dynamic phase of cellulose utilization during the early stages of incubation (Table 2).

Table 1
Cellulose addition.

Soil	Fertilization	C_{mic} (μg g^{-1} soil)	400% C-cellulose (μg g^{-1} soil)	Cellulose addition (mg 3.8 g^{-1} soil)
Dikopshof	Fertilized	155	622	5.4
Dikopshof	Unfertilized	70	280	2.4
Reckenholz	Fertilized	213	853	7.4
Reckenholz	Unfertilized	162	650	5.6
Thyrow	Fertilized	106	425	3.7
Thyrow	Unfertilized	31	126	1.1
QualiAgro	Fertilized	227	908	7.8
QualiAgro	Unfertilized	167	668	5.8

Table 2
Sampling schedule.

Analyses	Sampling time
CO_2 respiration	0, 4, 5, 8, 12, 16, 20, 26, 32, 43, 46, 56, and 64 d
^{13}C respiration	4, 8, 16, 32, and 64 d
$^{13}C_{mic}$	4, 8, 16, 32, and 64 d

A flowchart illustrating the experimental design as well as a nomenclature of important quantities and their units are provided in the supplementary material (Supplementary Fig. S1, Supplementary Table S1).

2.3. CO_2 measurement

Gas samples were taken from the incubation vials according to the experiment schedule (Tabel 2) to measure CO_2 accumulation between the sampling dates. In a first step, exetainers were flushed with CO_2-free air at the start of the experiment and after taking the head space samples at each sampling date. At the sampling dates (i.e. before flushing the vials with CO_2-free air), gas samples from the head space were transferred into exetainers (Labco, UK). The CO_2 concentration was quantified using a gas chromatograph (Agilent 7890, USA). To calibrate and calculate the CO_2 concentrations, three standard gases with known CO_2 concentrations were used. $^{13}CO_2$ was measured with a mass spectrometer (Thermo Finnigan MAT, Bremen, Germany). The at% of the CO_2–C respired between the sampling dates $t = i$ and $t = i + 1$ was calculated as follows:

$$at\% = \left(\frac{C_i \cdot at\%_i - C_{i+1} \cdot at\%_{i+1}}{C_i - C_{i+1}}\right) \quad (1)$$

where C_i and C_{i+1} are the CO_2–C concentrations and $at\%_i$ and $at\%_{i+1}$ the atom% of the CO_2–C at the respective sampling dates. The *at%* values of the evolved CO_2–C were taken to calculate the proportion of cellulose-derived C (%cellulose C) in CO_2–C at $t = i + 1$:

$$\%CelluloseC = \left(\frac{at\%_{sample} - at\%_{control}}{at\%_{cellulose} - at\%_{control}}\right) \cdot 100 \quad (2)$$

where $at\%_{sample}$ is the *at%* content of the sample, $at\%_{control}$ corresponds to the *at%* of the control soil, $at\%_{cellulose}$ refers to the *at%* of the added cellulose. As ^{13}C and CO_2 were not measured in the same interval, the missing *at%* values were estimated by linear interpolation between two time points. The respired CO_2 was partitioned based on the isotopic signature of the substrate and priming effect was calculated (Boos et al., 2023):

$$PE = CO_{2,total} - {}^{13}C - CO_2 - CO_{2,control} \quad (3)$$

where PE is the priming effect, $CO_{2,total}$ is the CO_2 evolved from the substrate enriched soil, $CO_{2,control}$ is the CO_2 evolved without substrate addition and $^{13}C - CO_2$ is the amount of labeled CO_2 evolved from the amended soil.

2.4. Bomb combustion calorimetry

The background energy content of the different soils was determined by combustion calorimetry and TG-DSC measurements. Following the methodological procedure described by Lorenz et al. (2024b), a subset of the homogenized soil was first dried at 105 °C and stored in a desiccator until combustion calorimetric measurements were performed. The energy content was determined as enthalpy of combustion $\Delta_C H$ according to DIN 51900 using an isoperibol combustion calorimeter (IKA C 200, IKA-Analysentechnik, Heitersheim, Germany; Lorenz et al., 2024b). In brief, 0.5 g of soil was mixed with benzoic acid in a 1:1 (w/w) ratio as an auxiliary combustion source and placed in a quartz crucible inside the bomb. This was done to achieve a complete combustion of SOM (Lorenz et al., 2024b). A volume of 5 ml of distilled water (25 °C) was added to the bomb to collect gases containing N and S from the combustion reaction to correct for energy releases by formation of nitric and sulfuric acid (for details see Lorenz et al., 2024b). The sealed bomb was pressurized with pure oxygen (purity 99.998 mol%, ALPHAGAZ) to 30 bar. After the combustion reaction, the residual material was weighed to account for the ash content of the analyzed sample. In case the combustion failed or was incomplete (recognizable by black soot in the sample residue), the respective measurement was discarded and repeated. Analysis of the C content in the combustion residues using an elemental analyzer (Vario EL cube, Elementar Analysensysteme GmbH, Langeselbold, Germany) confirmed that SOM had been completely burned in all samples. The combustion enthalpy is reported normalized to the organic C content (Lorenz et al., 2024a) of the sample in kJ g^{-1} C to better characterize the energetic signature of SOM, which is of particular importance for mineral soil samples.

2.5. Thermogravimetry-differential scanning calorimetry (TG-DSC)

The thermogravimetric and differential scanning calorimetric analyses were performed with STA 449 F3 Jupiter® simultaneous thermal analyzer equipped with type-S thermocouple (Pt–Pt/Rh) DSC/TG Octo sample carrier (Netzsch-Gerätebau GmbH, Selb, Germany) and coupled via a heated transfer line at 300 °C, untreated fused silica capillary, l = 2.2 m, d = 75 μm (SGE Analytical Science, Ringwood, Victoria, Australia) with the QMS 403 Aeolos® Quadro quadrupole mass spectrometer (Netzsch-Gerätebau GmbH, Selb, Germany). Samples were weighted in Al_2O_3 crucibles (d = 6.8 mm, V = 85 μL) on the Cubis® II Ultra-Micro lab balance (Sartorius AG, Göttingen, Germany). The sample mass was approx. 30 mg. An empty Al_2O_3 crucible was used as a reference. The samples were heated from 45 °C to 1000 °C at 10 °C min^{-1} under an oxidative atmosphere of 50 mL min^{-1} of synthetic air (N_2/O_2, 80/20 %) and 20 mL min^{-1} of Argon as a protective gas. The temperature and enthalpy calibration of the DSC was carried out at regular intervals. The performance of the TG unit was regularly checked by the thermal decomposition of calcium oxalate monohydrate. For the TG data, a correction measurement (blank value determination) was performed with an empty Al_2O_3 crucible under the same conditions to consider the influence of buoyancy on the thermobalance. Measurements were conducted in triplicates for each soil. Data evaluation was done by the Software NETZSCH Proteus Thermal Analysis (Netzsch-Gerätebau GmbH, Selb, Germany). The mass loss of soil organic matter m_{SOM} (in mg) in the sample was determined for the TG data. The heat of combustion Q_C (in J) was evaluated by combusting each replicate two times and subtracting the corresponding DSC curves (Fernández et al., 2011). A linear baseline was used to determine the Q_C from the DSC data according to (Barros, 2021). The combustion enthalpy of SOM in each soil is expressed as $\Delta_C H_{SOM}$ (in kJ g^{-1} SOM) or related to the carbon content (in kJ g^{-1} C).

2.6. Calorespirometry

Heat production rate was determined using a TAM Air (TA Instruments, New Castle, USA) isothermal heat conduction microcalorimeter with eight twin channels at an internal temperature of 20 °C. The set of calorimeter vials sampled at 64 days (see chapter 2.2) was used for continuous measurement of the heat production rate. The vials were removed from the calorimeter at the three aeration events. Each time the vials were (re-)placed in the calorimeter, a 45-min thermal equilibration period was applied before the heat signal was considered stable. Vials filled with water of the same heat capacity as the soil samples were used as a reference. The specific heat production rate $P(t)$ per gram soil is derived from Eqn. (4) (Yang et al., 2024):

$$P(t) = \sum_{i=1}^{n} r_i(t) \cdot \Delta_r H_i \tag{4}$$

where $r_i(t)$ is the rate of all i reactions (per gram soil) and their combined reaction enthalpies $\Delta_r H_i$ (Yang et al., 2024; Assael et al., 2022).

The specific heat ($Q(t)$; kJ g^{-1}) was determined by

$$Q(t) = \int_{t=0}^{t} P(t)dt \tag{5}$$

as the integrated specific heat production rate $P(t)$ (Yang et al., 2024).

The net energy use efficiency EUE_{net} was determined by dividing the cumulative heat production, including the utilization of cellulose and the priming of SOM, by the energy that was initially added via the cellulose and subtracting the result from 1. The EUE_{net}, therefore, provides a measure of how much energy the system gained or lost during the incubation. The equation for EUE_{net} is as follows:

$$EUE_{net} = 1 - \frac{Q(t)}{\Delta E_{cellulose}} \tag{6}$$

where $Q(t)$ is the specific heat per gram soil (Eqn. (5), and $\Delta E_{cellulose}$ is the total combustion enthalpy ($\Delta_C H$) of the added cellulose per gram soil (kJ g^{-1}).

The calorespirometric ratio (CR; kJ mol^{-1} CO_2–C) was calculated from the quotient of the cumulative, metabolic heat ($Q(t)$; kJ g^{-1} soil) and the cumulative CO_2 respiration ($R_{CO_2}(t)$; mol $CO_2 - C$ g^{-1} soil (Yang et al., 2024);):

$$CR = \frac{Q}{R_{CO_2}} \tag{7}$$

We also determined the enthalpy change according to Chakrawal et al. (2020) of the growth reaction on cellulose under aerobic conditions as a function of the relative degree of reduction (DR, γ) of cellulose and microbial biomass:

$$\Delta_r H_{cellulose} = \left(1 - Y_{cellulose}\frac{\gamma_{MB}}{\gamma_{cellulose}}\right)\Delta_C H_{cellulose} \tag{8}$$

where $\Delta_r H_{cellulose}$ is the reaction enthalpy of the growth reaction on cellulose and $\Delta_C H_{cellulose}$ is the combustion enthalpy of cellulose and $Y_{cellulose}$ is the yield coefficient for biomass formation. The relative degree of reduction of cellulose $\gamma_{cellulose}$ and microbial biomass γ_{MB} were calculated using

$$\gamma = \frac{4 \cdot n_C + n_H - 2 \cdot n_O - 3 \cdot n_N}{n_C} \tag{9}$$

where n_X is the number of atoms of X in the compound and CO_2, NH_3 and H_2O are assumed as the reference compounds with zero degree of reduction (Chakrawal et al., 2020). This equation yields $\gamma_{cellulose} = 4$ as well as $\gamma_{MB} = 4.284$ for an empirical biomass composition of $CH_{1.571}O_{0.429}N_{0.143}$ as recently suggested by Yang et al. (2024) for soil.

2.7. Microbial biomass (C_{mic})

Microbial biomass was determined using the chloroform fumigation

extraction method, originally introduced by Vance et al. (1987) and further modified by Poll et al. (2010) to allow additional quantification of ^{13}C. To quantify the ^{13}C content, 1.5 g of soil was fumigated (f) with ethanol-free chloroform for 24 h and then extracted with 6 mL of 0.025 M K_2SO_4. A non-fumigated (nf) 1.5 g control was extracted simultaneously. The difference in DOC concentration between the fumigated and non-fumigated sample corresponds to the microbial biomass C (extraction efficiency = 0.45). Since the quantification efficiency of the infrared detector of the TOC analyzer (Multi-N/C 2100S, Analytik Jena, Jena, Germany) decreases with increasing ^{13}C *at*% content, the data were corrected with a calibration curve ranging from 1 to 99 *at%*. $^{13}C_{mic}$ in μg C g^{-1} soil was determined by multiplying the total microbial biomass with the labeled microbial biomass (% $^{13}C_{mic}$ (Geyer et al., 2019);):

$$at\%C_{mic} = \left(\frac{at\%f \cdot fC_{mic} - at\%nf \cdot nfC_{mic}}{fC_{mic} - nfC_{mic}}\right) \quad (10)$$

$$at\%^{13}C_{mic} = \left(\frac{at\%_S - at\%_C}{at\%_{Cellulose} - at\%_C}\right) \cdot 100 \quad (11)$$

$$^{13}C_{mic} = \frac{C_{mic} \cdot at\%^{13}C_{mic}}{100} \quad (12)$$

where the organic carbon content of the fumigated and non-fumigated samples (μg C g^{-1} soil) was expressed as fC_{mic} and nfC_{mic}, while the corresponding ^{13}C atom% values were labeled as *at%f* and *at%nf*. $at\%_S$ and $at\%_C$ represent the atom percent of sample treatments and the natural abundance in the soil, respectively. $at\%_{Cellulose}$ represents the atom percent of the cellulose.

2.8. C use and storage efficiency

The CUE was derived from the ^{13}C mass balance, and from the calorespirometric ratio.

1. CUE_L: experiment-based CUE used for labeled substances (Geyer et al., 2016).

$$CUE_L = \frac{^{13}C_{mic}}{^{13}C_{mic} + {}^{13}CO_2} \quad (13)$$

where: $^{13}C_{mic}$ is the C uptake in microbial biomass, and $^{13}CO_2$ is the cumulated mineralized cellulose-derived C.

2. CUE_{Rq}: calorespirometric ratio (CR)-based CUE.

$$CUE_{Rq} = \left(\frac{406\left(1 - \frac{Ox_{cell}}{4}\right) - \frac{Q}{R_{CO_2}}}{115(Ox_{cell} - Ox_{MB})}\right) \cdot \left(\frac{406\left(1 - \frac{Ox_{cell}}{4}\right) - \frac{Q}{R_{CO_2}}}{115(Ox_{cell} - Ox_{MB})} + 1\right)^{-1} \quad (14)$$

where 406 (kJ mol^{-1} O_2) is the combustion enthalpy of cellulose, Ox_{cell} - Ox_{MB} is the difference between the oxidation states of C in the substrate (cellulose = 0; Saito et al. (2007)) and in the microbial biomass (−0.3; Von Stockar and Liu (1999)) and 115 is the average energy loss (kJ) per change in oxidation state of C during the conversion of substrate to microbial biomass (Geyer et al., 2019; Kemp, 2000).

3. CB_{net}: net carbon balance including C released from cellulose and SOM:

$$CB_{net} = 1 - \frac{C_{CO_2}}{C_{cellulose}} \quad (15)$$

where C_{CO_2} is the total cumulative CO_2 release (μg C g^{-1} soil) and $C_{cellulose}$ is the total amount of carbon added to the soil in the form of cellulose (μg C g^{-1}). CB_{net} thus measures the net retention ($CB_{net} > 0$) or loss ($CB_{net} < 0$) of C in the soil after substrate addition. Note that $CB_{net}(t = 0) = 1$ and that CB_{net} decreases over time.

2.9. Data analyses

All data analyses were carried out using the statistical software R 4.0.2 (R Core Team, 2020). Significant differences were tested using a linear mixed-effects model with C_{mic}^{13}, CO_2^{13} and heat production rate as dependent variables and time, fertilizer status and experimental sites as explanatory variables. Models were fitted to the data using the "lme4" package (Bates et al., 2008). For the $^{13}CO_2$ data, we integrated the time factor for repeated measurements by crossing it with the treatment structure, including an interaction effect between site and site-time point and a random effect of the individual microcosms in which the CO_2 measurement took place (Piepho et al., 2004). We carried out a three-way anova to identify significant effects ($p < 0.05$) and then compared the estimated marginal means. Normal distribution and variance homogeneity were tested by means of residual diagnostic plots. If an interaction with time point was significant, we evaluated simple contrasts per time point level.

2.10. Dynamic model

We simulated the coupled fluxes of carbon and energy with an ordinary differential equation (ODE) model of microbial growth after the addition of ^{13}C-labeled cellulose. The model is based on similar formulations by Chakrawal et al. (2020, 2021) and Endress et al. (2024a), which were extended to represent ^{13}C dynamics. In total, the model features 5 major carbon pools including the concentrations of substrate (^{13}C-cellulose) as well as microbial biomass and CO_2, each with separate pools for ^{12}C and ^{13}C. In the model, microorganisms grow aerobically on the added ^{13}C-cellulose following Monod kinetics with a threshold concentration, forming new ^{13}C-biomass as well as ^{13}C–CO_2. To capture potential priming, microbes also utilize native soil ^{12}C-SOM to form new ^{12}C-biomass and ^{12}C–CO_2 via a second aerobic growth reaction. Model SOM is characterized by its average degree of reduction γ_{SOM}, which is incorporated as a free parameter. Counteracting the growth reactions, total biomass ($^{12}C + {}^{13}C$) is constantly consumed to fuel endogeneous maintenance respiration, releasing both ^{12}C- and ^{13}C–CO_2, and finally gets turned over to necromass at a specific rate.

In addition to the distinction between ^{12}C- and ^{13}C-biomass, the model also partitions the total biomass into an active fraction, which performs both growth and maintenance reactions, as well as an inactive fraction, which only performs maintenance. Changes in the activity state are modeled via the index of physiological state framework and depend on the availability of cellulose as the primary substrate (Panikov, 1996; Blagodatsky and Richter, 1998). Note that this partitioning implies that the same proportion of ^{12}C- and ^{13}C-biomass is considered active at any time.

This ODE model was implemented in Python (version 3.9.18) and numerical integration was carried out using the Radau method of the solve_ivp function in the Scipy package (Virtanen et al., 2020). The model was calibrated against the measured pools of total and ^{13}C-biomass, cumulative total and ^{13}C–CO_2, as well as the heat production rate. Parameter optimization was performed for each individual soil, i.e., we obtained eight calibrated parameter sets in total for the fertilized and unfertilized soils of the four field experiments. The optimization was carried out numerically using the Levenberg-Marquardt algorithm as implemented in the minimize function of the lmfit package (Newville et al., 2023). Initial conditions for substrate and biomass concentrations were chosen according to the measured experimental values and lower and upper bounds were provided for individual parameters. The full ODE model as well as a detailed description of the

calibration routine is presented in the supplementary materials and methods (SI Text). A list of all variables and parameters with units is given in the supplementary material (Supplementary Table S4).

3. Results

3.1. $^{13}C_{mic}$ content and $^{13}CO_2$ release

The $^{13}C_{mic}$ content began to increase after 3 days and was comparable in its dynamics for all soils and fertilizer status. Averaged over the fertilization status, since we observed no significant difference, the maximum $^{13}C_{mic}$ content at day 16 ranged from 20 μg g^{-1} soil at TH to 100 μg g^{-1} soil at QA (Fig. 2a–d; dashed lines), i.e. there was a significant increase from the baseline value of about 0.0017 μg g^{-1} soil on day 0 ($p < 0.05$; Fig. 2a–d).

This increase corresponds to approximately 10% (TH) and 20% (QA) of the initially added cellulose-C. After day 16, growth was counterbalanced to some extent by continued ^{13}C losses from the biomass pool and fell back to baseline by day 64 (Fig. 2a–d). Microbial growth was accompanied by an sigmoidal increase in cumulative $^{13}CO_2$ release, whereby after a lag phase of about 3 days, an exponential phase occurred until day 16, which then turned into a saturation phase (Fig. 2e–h; dashed line). The statistical comparison of the cumulative $^{13}CO_2$ release at the end of incubation showed no statistical difference between the fertilized and unfertilized treatment and ranged on average from TH-UF with 22.5 ± 11.7 to 261.2 ± 131.7 μg g^{-1} soil in RE-FYM (Fig. 2e–h). The general increase in biomass (C_{mic}) and respiration (CO_2) evolved at a comparable rate as the ^{13}C content (Fig. 2; solid lines).

3.2. Priming effect

The percentage of labeled cellulose-C in relation to the total CO_2 release, corrected for the CO_2 coming from the control soil, ranged from 37% (TH-UF) to 79% (RE-FYM) on day 64. After cellulose application, we observed a positive priming effect in all soils. PE started to increase immediately after cellulose application and was higher in the fertilized soils and in the soils with a higher C content (QA, RE). In the fertilized soils, the PE ranged from 74.5 μg g^{-1} soil (TH) to 182.9 μg g^{-1} soil (QA). At the unfertilized sites, PE ranged from 38.4 to 131.7 μg g^{-1} soil in the same order. The priming effect as a percentage of C added as cellulose showed an inverse pattern compared to the total amount of primed C, with values ranging from 10% in the RE-FYM to 32% in the TH-UF (Fig. 3).

3.3. Combustion enthalpy of SOM

The combustion enthalpy determined by combustion calorimetry in the unfertilized variants tended to be higher than in the fertilized soils, ranging from 436 ± 143 kJ $mol^{-1}C$ in QA to 732 ± 30 kJ $mol^{-1}C$ in TH. In the fertilized soils, the energy content ranged from 306 ± 106 in DI to 439 ± 21 kJ $mol^{-1}C$ in TH. TH-UF was therefore the soil with the highest SOM combustion enthalpy according to combustion calorimetry (Supplementary Fig. S3, Table S5). Combustion enthalpy values determined by TG-DSC tended to be higher than those determined by combustion calorimetry, but followed the same pattern across soils. The energy content ranged from 397 ± 12 kJ $mol^{-1}C$ in QA to 820 ± 181 kJ $mol^{-1}C$ in TH for the unfertilized soils and from 407 ± 177 kJ $mol^{-1}C$ in QA to 609 ± 40 kJ $mol^{-1}C$ in TH in the fertilized soils. Thus, TH-UF was also the soil with the highest SOM combustion enthalpy when determined via TG-DSC.

3.4. Heat production rate and specific heat

The heat production rate P_t increased exponentially without any significant lag phase, peaking after about eight days and falling back to the initial value after about 20 days, indicating that growth took place up to day eight (Fig. 4a; the apparent specific growth rate is included in Supplementary Fig. S5). On fertilized sites, the maximum P_t ranged from the lowest value at DI with 7.0 ± 1.7 μW g^{-1} to the highest value of 21.73 ± 2.2 μW g^{-1} (Fig. 4a–d) at RE, which was reached after eight to ten days. In the unfertilized soils, P_t at the maximum was significantly reduced in RE and QA ($p < 0.01$) and peaked at 14.73 ± 1.56 μW g^{-1} (−32.21%) and 12.50 ± 1.5 μW g^{-1} (−23.8%).

In TH and DI there was no statistically significant difference between

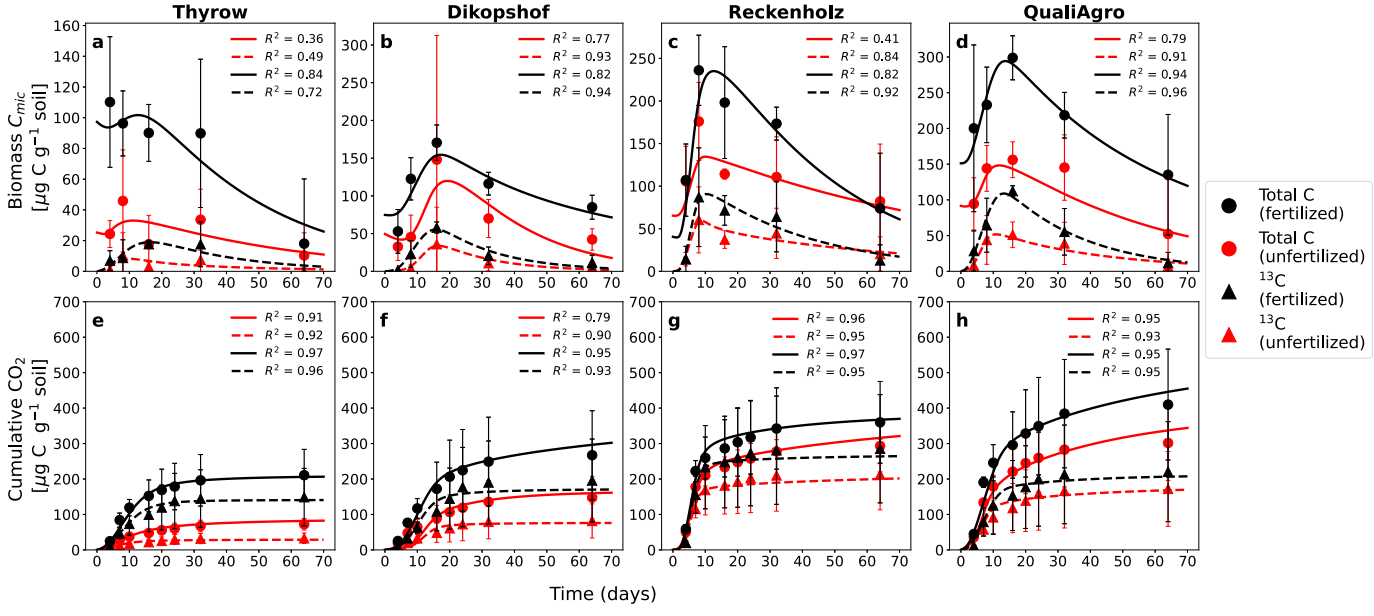

Fig. 2. Microbial biomass content (C_{mic}, **a-d**) and cumulative CO_2 release (**e**–**h**) of all soils. Dots and solid lines correspond to total C measurements and model fits, respectively. Triangles and dashed lines correspond to ^{13}C measurements and model fits. Results for the fertilized soils are shown in black, results for unfertilized soils are shown in red. Data shown represent mean values and standard deviation ($n = 3$). (For interpretation of the references to colour in this figure legend, the reader is referred to the Web version of this article.)

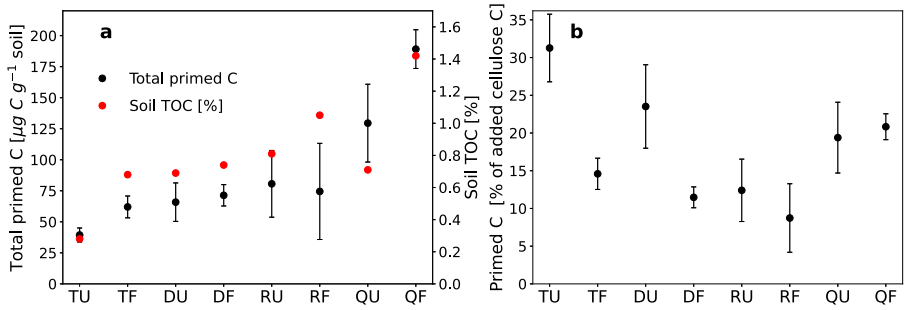

Fig. 3. Observed priming effect after cellulose addition. **a** Total primed C as measured by cumulative ^{12}C–CO_2 release (black). Soil TOC (%) as reported by Lorenz et al. (2024a) is shown in red (note the second y-axis). **b** Priming effect expressed as a percentage of C added as cellulose. Data shown represent mean values and standard deviation ($n = 3$). (For interpretation of the references to colour in this figure legend, the reader is referred to the Web version of this article.)

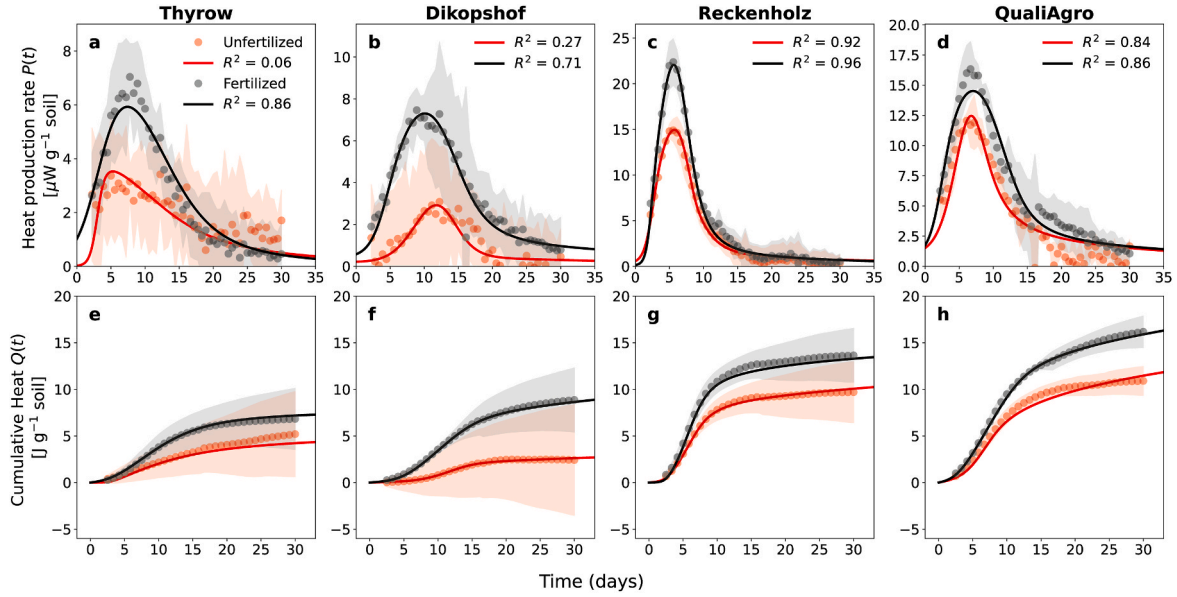

Fig. 4. Heat production rate P_t (**a**–**d**) and cumulative heat Q_t (**e**–**h**) for all soils (black dots = fertilized, red dots = unfertilized). The corresponding lines represent the mechanistic model fit. Shaded areas represent standard deviation ($n = 3$). (For interpretation of the references to colour in this figure legend, the reader is referred to the Web version of this article.)

fertilized and unfertilized soils. In these less active soils, in which we could not observe this increase up to about 20 μW g^{-1}, the TAM Air operated at the detection limit (0–10 μW g^{-1}, based on the fluctuations in the measurement of the heat production rate) even in the phase of exponential increase between three and eight days, which is reflected in the higher standard deviation (Fig. 4a–d). The same dependence on fertilization status as observed for P_t was also observed for the specific heat Q_t (Fig. 4e–h). After 30 days, 16.5 ± 2.1 J g^{-1} and 13.8 ± 3.4 J g^{-1}

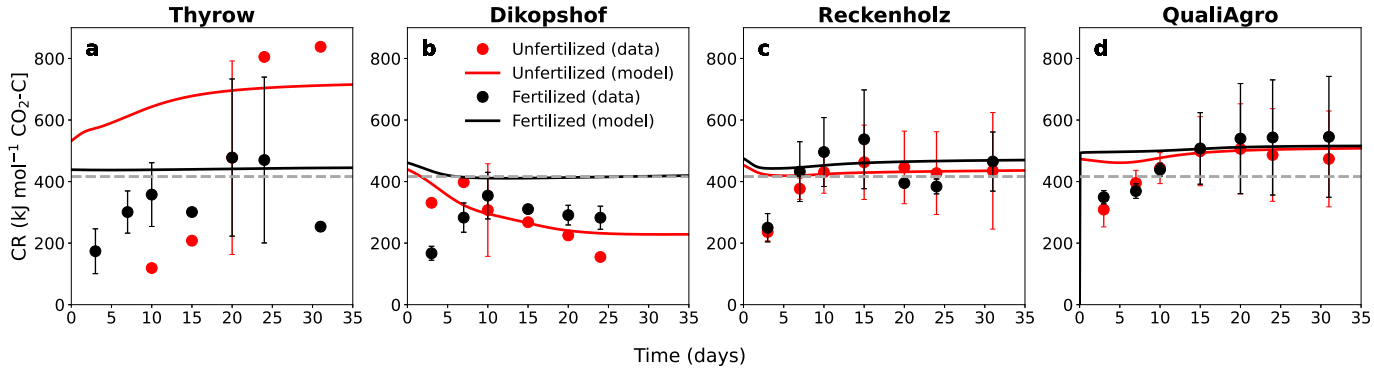

Fig. 5. Calorespirometric ratio over 35 d following cellulose amendment for all soils (black = fertilized, red = unfertilized). The dotted line is the expected calorespirometric ratio upon complete oxidation of cellulose (406 kJ mol^{-1} CO_2–C). Dots correspond to the measured data and respective lines represent the output of the mechanistic model. Data shown represent mean values and standard deviation ($n = 3$). (For interpretation of the references to colour in this figure legend, the reader is referred to the Web version of this article.)

were attained in QA-FYM and RE-FYM, whereas only 11.2 ± 1.7 (−32%; $p < 0.01$) and 9.8 ± 5.2 J g^{-1} (−29%; $p < 0.01$) were reached at the unfertilized sites (Fig. 4e–h). Again, due to the measurement uncertainty of the heat production rate in TH and DI and the resulting high standard deviation (Fig. 4e–h), no significant difference between the fertilized and unfertilized treatments could be determined.

3.5. Calorespirometric ratio

The CR calculated from the ratio of cumulative heat production and respiration started to increase during the exponential growth phase (0–16 days) from about 250 to about 540 kJ mol^{-1} at least for QA and RE, regardless of the fertilization status (Fig. 5).

At DI and TH, this relationship between heat production and respiration was more difficult to establish, due to the low general activity, making it difficult to correctly determine the heat production. Once more, this is reflected in a high standard deviation. Nevertheless, the pattern of increase was still discernible, but the value of 700 kJ mol^{-1} achieved in the unfertilized TH is exceptionally high (Fig. 5).

3.6. C and energy use and storage

The metrics describing C and energy use and storage in the soils were only calculated up to 32 days, because at this point the heat production rate approached very low levels, increasing the uncertainty of the data. When considering the net carbon balance over time, there was a decrease of CB_{net} from its initial value of 1 down to 0.5–0.7 (Fig. 6). The EUE_{net} showed almost identical dynamics, also falling from around 1 on day 0 to around 0.55 on day 32 (Fig. 6).

When the net balance measures CB_{net} and EUE_{net} were compared with CUE_L and CUE_{Rq}, CB_{net} and EUE_{net} were significantly higher ($p < 0.001$) during the first days (day 0 - day three). Over time, the CUE_{Rq} derived from the calorespriometric ratio at times exceeded the CB_{net} and EUE_{net}, but the CUE_L was always lower than the net C and energy balance. CUE_{Rq} decreased until days eight and ten down to 0.19 to 0.65 in most of the soils. It should be noted that Eqn. (14) does not permit to estimate the CUE_{Rq} for CR values above 406 kJ mol^{-1}, which substantially reduced the number of CUE_{Rq} estimates. CUE_L was between 0.3 (DI-UF) and 0.71 (QA-FYM) on day four. As expected, the CUE_L decreased after day 16 when the concentration of labeled biomass had peaked on day 16 while $^{13}CO_2$ losses continued (Fig. 6).

In addition to analyzing CR as a function of time (Fig. 5), we describe here the relationship between CUE_L and CR (Fig. 7).

We use CUE_L, because CUE_{Rq} is directly derived from the CR and therefore not a CR-independent measure of CUE. The two components of the CR (heat and CO_2 release rates) vary to different degrees and therefore allow conclusions to be drawn about C or energy limitation of microbial growth. Specifically, CR values that decrease with CUE and are limited to below the combustion enthalpy of biomass (≈485 kJ mol^{-1}C using our assumptions) are taken to indicate energy limitation, whereas CR values that increase with CUE and are limited to values above this threshold are taken to indicate C limitation of growth (Fig. 7). CUE was found to decrease with increasing CR up to day eight across soils. When CUE is at its maximum, about 0.5–0.75, and not much heat is released, CR is lowest in the range of 200–300 kJ mol^{-1}. On the contrary, when growth stops (i.e. CUE ≈0.18 to 0.25 after 32 days), CR is maximised. On the other hand, we also observed CR values around or exceeding the combustion enthalpy of cellulose (406 kJ mol^{-1}C) and biomass (485 kJ mol^{-1}C), in particular during the later stages and in the SOM rich soils of RE and QA (Fig. 5). This can be explained by the use of an additional energy and C-source such as SOM that is more reduced than cellulose and would correspond to C limited growth in these instances.

3.7. Model behavior and performance

The dynamic model adequately reproduced the time series of CO_2 and heat production as well as biomass growth and turnover over the course of the incubation for all soils. In particular, the simulated combination of growth reactions using either added ^{13}C-cellulose or native ^{12}C-SOM as substrates properly captured the dynamics of both ^{12}C and ^{13}C pools (Fig. 2). Moreover, the sum of their corresponding heat contributions was in good agreement with measured total heat production rate (Fig. 4), although the experimental results showed high variance in the SOM-poor soils (TH and DI).

This close coupling of carbon and energy release was also reflected in the simulated CR, which was generally aligned with experimental estimates, especially in the SOM-rich soils (RE and QA, Fig. 5). Overall, the

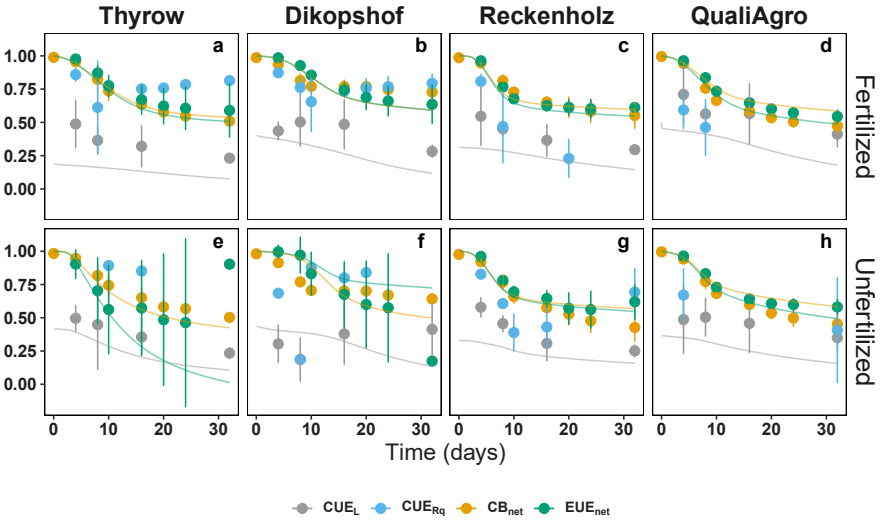

Fig. 6. C use efficiency and net C and energy balances during the incubation for the fertilized (**a**–**d**) and unfertilized (**e**–**h**) soils. Grey represents the CUE derived from the labeled C (CUE_L), blue the CUE based on the CR (CUE_{Rq}), and orange the net carbon balance (CB_{net}). Green represents the net energy use efficiency (EUE_{net}). The corresponding lines indicate the respective outputs of the mechanistic model. Data shown represent mean values and standard deviation ($n = 3$). For CUE_{Rq}, only values derived from CR < 406 kJmol^{-1} are shown. (For interpretation of the references to colour in this figure legend, the reader is referred to the Web version of this article.)

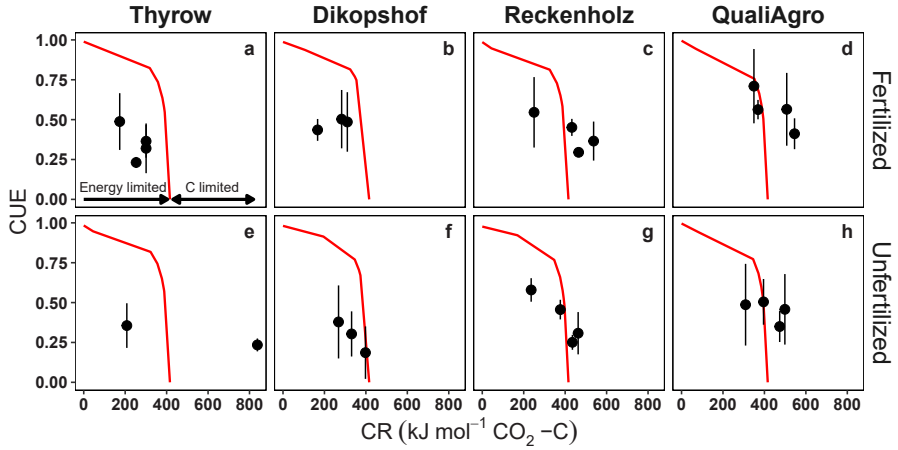

Fig. 7. CUE_L as a function of CR (black dots) for the fertilized (**a**–**d**) and unfertilized (**e**–**h**) soils. In TH and DI there are lacking data points due to the missing $^{13}CO_2$ determination. The total enthalpy change of cellulose metabolism ($\Delta_i H_{cellulose}$; red line) can be described as a function of the degree of reduction for both cellulose and the microbial biomass ($\gamma_{cellulose} = 4$, $\gamma_{MB} = 4.284$). Data shown represent mean values and standard deviation ($n = 3$). (For interpretation of the references to colour in this figure legend, the reader is referred to the Web version of this article.)

cumulative model CR showed less temporal variation than the observations and was instead dominated by its value during the growth phase. The two soils with the lowest SOM content, i.e., the unfertilized soils of TH and DI, were an exception to this, with cumulative CR increasing and decreasing from its initial value over time, respectively.

As suggested by the close model fit to the cumulative data, CB_{net} and EUE_{net} as well as ^{13}C-CUE_L estimates obtained from simulations resembled their experimental counterparts (Fig. 6). In addition to these directly obtainable experimental measures, model simulations also allowed the estimation of ^{12}C-CUE_L, i.e., modeled $^{12}C_{mic}$ formation relative to modeled SOM consumption, as well as total CUE_L, i.e., modeled net C_{mic} formation relative to the combined modeled consumption of cellulose and SOM (Supplementary Fig. S4). These modeled measures showed generally lower (TH, QA) or similar (DI, RE-UF) $^{12}C-CUE$ relative to $^{13}C-CUE$, with the exception of RE-FYM, where growth on SOM was modeled as more efficient. The analysis also revealed a temporal pattern of biomass formation being first fueled by cellulose consumption, followed by later contributions due to SOM utilization (Supplementary Fig. S4). In terms of net growth, the experimental cellulose amendment resulted in an increase in total C_{mic} after 32 days in all soils except TH, where biomass levels dropped to (TH-UF) or below (TH-FYM) their initial values within that time span (Fig. 2a–d).

In terms of the calibrated parameter sets, optimized values indicated that specific growth rates μ_{max} fueled by cellulose exceeded those fueled by SOM in all soils (Supplementary Fig. S5), and μ_{max} was higher in the unfertilized soil for all sites except RE, where this trend was reversed. Finally, the modeled degree of reduction γ_{SOM} of the consumed SOM were in good agreement with experimental measurements derived from the average energy content of the bulk SOM determined via bomb calorimetry and TG-DSC in most soils (Supplementary Fig. S3, Fig. S6). QA and DI-UF presented notable exceptions, with higher (QA) and lower (DI-UF) values compared to experimental estimates, respectively.

4. Discussion

It is established that the CUE, CR and microbial growth kinetics can be reliably derived from calorespirometric measurements for growth on rapidly metabolized substrates, especially under aerobic conditions (Yang et al., 2024; Von Stockar et al., 2006; Barros et al., 2000; Chakrawal et al., 2020). In the following, we will discuss to what extent CR is related to microbial growth on added cellulose as a slowly degradable substrate compared to glucose, how a possible priming of SOM affects CR and how the measurement accuracy of calorimetry affects CUE and EUE_{net} estimates as well as CR compared to the determination of microbial CUE by other methods. Finally, we address technical issues that arise when combining the energy and carbon flow in the CR framework.

4.1. The CR reflects the coupling of energy and carbon flux during microbial growth after cellulose amendment

Across the studied soils, our observed CR values in the range of 200–540 kJ mol^{-1} CO_2–C are broadly consistent with aerobic growth on cellulose. They are comparable to the findings of previous studies that reported CR values during microbial growth on glucose with yields of 0.5–0.75, characteristic of highly efficient aerobic growth (Hansen et al., 2004; Chakrawal et al., 2021). Since glucose units form the primary structure of cellulose, the metabolic processes involved in microbial growth on these substrates are very similar, apart from the hydrolysis required for the extracellular depolymerization of the cellulose (Blagodatskaya et al., 2014; Popovic et al., 2019; Sørensen et al., 2015; Datta et al., 2017). Given this context, the theoretical framework proposed by Chakrawal et al. (2020) for the variation of the CR of different metabolic pathways of glucose (and SOM) utilization can be applied to our data. The principal distinction is that we measured a combustion enthalpy of $\Delta_c H_{cellulose} = 406$ kJ mol^{-1} C for the cellulose used in this study, in contrast to the literature value of $\Delta_c H_{glucose} = 469$ kJ mol^{-1} C for glucose. If the growth reaction fueled by cellulose was the only process contributing to observed CO_2 and heat production, the range of possible CR values would be fully determined by this combustion enthalpy along with the microbial CUE and the degree of reduction γ_{MB} of the newly formed microbial biomass (Eqn. (14)). Assuming a biomass composition of $C_1H_{1.571}O_{0.429}N_{0.143}$ as suggested for soils in this context (Yang et al., 2024), cellulose represents a more oxidized substrate relative to biomass, i.e., $\gamma_{cellulose} < \gamma_{MB}$, and the growth reaction is characterized by a decrease in CR for increasing CUE (Fig. 7), with a maximum of $CR = \Delta_c H_{cellulose} = 406$ kJ mol^{-1} C for pure catabolism (i.e., CUE = 0, Kästner et al., 2024). Minor deviations from this predicted CR-CUE relationship may be attributed to variations in the actual biomass composition and thus in γ_{MB} as noted by Chakrawal et al. (2020). However, we observed CR values well above and below this theoretical prediction (Fig. 7). Yang et al. (2024) also reported an average CR of 577.7 kJ mol^{-1} C obtained from cumulative heat measurements and 567.6 kJ mol^{-1} C obtained from the corresponding heat production rate after glucose addition to the DI-FYM soil, well above their theoretical predictions, and pointed to additional SOM utilization or partial anoxic conditions as potential explanations of this

observation. Our results using labeled ^{13}C-cellulose confirmed such substantial SOM utilization over the course of the incubation and associated observed deviations from the predicted CR-CUE curve. Critically, this predicted CR-CUE relationship is only applicable to the pure growth reaction on cellulose, and will be altered by additional contributions of heat and CO_2 from the growth reaction fueled by SOM, which is characterized by its own degree of reduction and yield coefficient. Following Chakrawal et al. (2020), the simple relationship predicted for cellulose corresponds to energy limited microbial growth, which releases relatively more C than heat as efficiency increases. In our data, we observe this pattern only during the early stages of the incubation across soils (at least up to day eight after substrate addition). However, this pattern is no longer evident later during the incubation, especially in the SOM-rich soils and in TH-UF (Figs. 5 and 7). For all of these soils, our model predicts the utilization of more reduced SOM (Supplementary Fig. S6) that corresponds to C-limited growth in this framework, and our findings could thus be interpreted as an increasing contribution of SOM utilization after the cellulose addition in these soils.

In addition, we observed no net growth and lower activity for a large fraction of the later stages of our incubations (Figs. 2 and 4). If no further growth occurs during this time, the observed CO_2 and heat production will primarily result from maintenance and turnover processes (Manzoni et al., 2012) and thus again deviate from the CR of the growth reaction. In our dynamic model formulation, this slow conversion of biomass to CO_2 and heat due to maintenance predicts a CR of ≈490 kJ mol^{-1} C equal to the combustion enthalpy of microbial biomass (Chakrawal et al., 2020), which is in good agreement with the observed values especially in the SOM-rich soils (RE and QA, Fig. 7). However, future studies will benefit from a more nuanced consideration of the carbon and energy flux due to maintenance and turnover during the retardation and onset of starvation following the growth phase.

In principle, deviations of the CR from predictions for the aerobic growth reaction may also be caused by anaerobic metabolism (Chakrawal et al., 2020; Endress et al., 2024a; Barros et al., 2016). However, total O_2 concentration was not limiting in our vials, as the observed CR deviations occurred in incubations that differed strongly in the amount of added C and cumulative CO_2 release. Similarly, the formation of substantial anoxic microsites seems unlikely given the slow rate of cellulose decomposition in our samples, whereas such sites might be important in the case of more labile substrates and in natural, intact soils (e.g., Lacroix et al. (2022); Keiluweit et al. (2016)).

4.2. ^{13}C-labeling and dynamic modeling reveal a substantial priming effect

We observed a substantial PE after cellulose addition across soils, which cover a wide range of SOM contents (Tables S1 and S2) as well as total rates of C addition (Table 1) and were deliberately chosen for this study. The release of ^{12}C–CO_2, presumably fueled by the degradation of native SOM, accounted for a large share of total CO_2 emissions in all of these soils (Fig. 3). In absolute terms, the observed PE is consistent with the relationship described in the literature between the input of ^{13}C-labeled plant residues and the primed CO_2 − C (Blagodatskaya et al., 2014; Perveen et al., 2019). Blagodatskaya et al. (2014) ascribed the pronounced increase in the amount of active microbial biomass that occurs during the intensive phase of cellulose degradation to the elevated enzyme activity for the hydrolysis of chitin, cellulose and hemicellulose, which are also involved in the decomposition of SOM. While the absolute amount of primed C showed the expected relationship of increasing PE with native SOM content and amount of added cellulose across soils (Fig. 3), the PE relative to the amount of added C showed a more variable pattern (Fig. 3), ranging from 8.7% (RE-FYM) to 31% (TH-UF). In particular, the amount of degraded SOM per added substrate was strongly elevated in the unfertilized variants of the SOM-poor soils at TH and DI when compared to their fertilized variants ($p < 0.05$), whereas no such difference was observed in the SOM-rich soils. While the C content in the fertilized soils is always slightly higher compared to the unfertilized counterparts for all sites, this is not true for the C/N ratios (Tables S1–S2). Nevertheless, a C/N ratio of 7–9 indicates a good nutrient supply in all soils. It is conceivable that the fertilisation effect of farmyard manure could be partly offset, as Arcand et al. (2017) noted that the long-term application of organic material (e.g. straw) can reduce the N availability. As a result, in addition to the joint decomposition of soil organic matter and cellulose, additional N mining could have been stimulated, with potential further release of CO_2 and heat (Arcand et al., 2017; Chakrawal et al., 2021).

Combining the measured heat production with the carbon-based considerations offers further insights into the nature of the degraded SOM. Specifically, our observed CR values are consistent with substantial priming, given the deviations from predictions for the simple aerobic growth reaction fueled by cellulose. For example, an elevated CR, in particular above ≥406 kJ mol^{-1} C, would indicate heat and CO_2 contributions from the degradation of relatively reduced, energy-rich SOM, whereas low CR values might indicate the utilization of more oxidized and energy-poor SOM (Chakrawal et al., 2020; Barros, 2021). We observed both comparatively high and low CR values over the course of the incubation experiments, potentially reflecting the varying energy contents of SOM in the studied soils, which ranged from 305 to 732 kJ mol^{-1} C when determined via combustion calorimetry and from 397 to 820 kJ mol^{-1}C when determined via TG-DSC (Supplementary Fig. S3). More specifically, the parameter calibration of the dynamic model suggested a degree of reduction of the SOM consumed by microbes that is consistent with the measured energy contents of the bulk SOM (e.g., in the RE and TH soils as well as in DI-FYM, Supplementary Fig. S6). The TH-UF soil, which is characterized by both the lowest organic carbon content (Supplementary Table S2, Table S3) as well as the highest SOM energy content (Supplementary Fig. S3, Table S5) of all soils, provides a compelling illustration, with the model suggesting an extremely high $\gamma_{SOM} \approx 7$ that is in line with our experimental results (Supplementary Fig. S6). This soil also showed the most pronounced CR deviation, consistent with microbial utilization of such highly reduced SOM (Fig. 5). In contrast, we found discrepancies between the measured energy content of the bulk SOM and the modeled γ_{SOM} of microbially consumed SOM in some of the other soils. In the QA soils, the microbially degraded SOM was predicted to be more reduced than measurements of bulk energy contents would suggest, whereas the opposite was true in the DI-UF soil (Supplementary Fig. S6). In both cases, these discrepancies are consistent with observed CR deviations (Fig. 5) and may indicate a preferential use of SOM components that differ from the bulk SOM in terms of their average DR, although our data are insufficient to test this interpretation.

4.3. CUEs are indicative of cellulose metabolism, while CB_{net} and EUE_{net} reflect the balance of C and energy after the cellulose application

Our experimental and modeling evaluation of various estimators for the fate of substrate-derived C and energy revealed systematic differences between these approaches as well as their respective limitations. The interpretation of CUE based on ^{13}C-labeled substrates strongly depends on the considered time scale. While the efficiency of the immediate substrate use is reflected by the population CUE, the ecosystem CUE also considers processes such as microbial recycling at a longer time scale and is usually declining with time compared to the population CUE (Geyer et al., 2016). Notably, the ^{13}C-based CUE_L (Eqn. (13)), which we consider to be the most direct estimate, consistently yielded lower efficiencies than the other methods, ranging from 0.18 to roughly 0.7 and the decrease over time and across soils reflects the transition from the population to the ecosystem CUE. Nonetheless, these values indicate efficient aerobic growth in all incubations, and a lower efficiency than obtained for growth on more labile substrates such as glucose can be expected for the more complex cellulose (Manzoni et al., 2018; Öquist et al., 2017).

Efficiency estimates based on CUE_{Rq} (Eqn. (14)) turned out to be problematic. First and foremost, its derivation rests on the assumption that the CR primarily reflects the CO_2 and heat production of the aerobic growth reaction fueled by the added substrate (Hansen et al., 2004; Geyer et al., 2019). Yang et al. (2024) recently questioned whether this condition was met even in the case of glucose amendment, and it was certainly not met in our experiment, where we observed substantial SOM decomposition as well as substantial periods primarily characterized by maintenance and turnover processes. Accordingly, we obtained CR values (namely, CR $>$ 406 kJ mol^{-1} C) that Eqn. (14) maps to nonsensical (<0 or >1) CUE estimates for several time points in many of our incubations, as did Yang et al. (2024) in their recent experiments with glucose. Moreover, CUE_{Rq} estimates in the interval between 0 and 1 may still not reflect the actual growth efficiency due to, e.g., the impact of SOM utilization. For example, low CR values in the range of 200 kJ mol^{-1} C (e.g., as seen in the TH and DI soils, Fig. 5) correspond to a CUE_{Rq} exceeding ≈0.9. Such values would indicate that the C is channelled almost exclusively to anabolism (Geyer et al., 2016), which is beyond the physiological limits imposed by the energy demands of these reactions that need to be fueled by corresponding catabolism (Chakrawal et al., 2020). Similarly, biosynthesis is only possible when growth-independent energy requirements are met and a sufficient surplus of C and energy is available (Ingraham et al., 1983). Overall, maximum efficiency is limited to around 0.85 by respiration losses, even for the most reduced and energy-rich compounds (Gommers et al., 1988). Another example of an implausible pattern predicted by CUE_{Rq} can be seen in the DI-UF soil, which is characterized by consistently decreasing CR values that are mapped to increasing CUE estimates over time by Eqn. (14), in contrast to the ^{13}C-based CUE_L and the growth dynamics seen in the biomass time series (Fig. 2a–d). Overall, we conclude that CUE_{Rq} is only an appropriate estimator of growth efficiency if the underlying CR values can be reasonably assumed to primarily reflect the growth reaction on the added substrate. Accordingly, we observed the best agreement of this estimate with CUE_L during the phase of intense, cellulose-fueled growth, at least in the SOM-rich soils (RE and QA, Fig. 6).

The susceptibility of CUE_{Rq} to processes such as priming translates to CB_{net} (Eqn. (15)) and EUE_{net} (Eqn. (6)), which can be considered as storage efficiencies of the whole soil system (Manzoni et al., 2018) and are purely based on the cumulative release of CO_2 and heat, respectively. They continuously decreased from their initial value of 1 over the course of the experiment (Fig. 6), reflecting a continuous loss of C and energy. Notably, the use of ^{13}C-labeled cellulose enabled us to disentangle the contributions of substrate and SOM degradation to the loss and storage of both C and energy over the course of a long incubation using cellulose as a less degradable substrate. This revealed substantial priming and preferential use of SOM (Supplementary Fig. S6), but also retention of undecomposed cellulose across soils, highlighting the potential of combining ^{13}C- and energy based metrics as emphasized by Kästner et al. (2024). Both storage metrics can parallel CUE in the case of rapidly metabolized substrates such as glucose, which are quickly and completely converted to microbial biomass, CO_2 and heat (Hagerty et al., 2018; Wang and Kuzyakov, 2023; Yang et al., 2024; Endress et al., 2024a). For example, glucose may be taken up by microbial cells within few minutes without being immediately metabolized (Geyer et al., 2019). In such a case, both metrics would be close to 1 and start to constantly decrease while the glucose is being metabolized. However, it is important to consider that CUE focuses on the efficiency of the anabolic use of the substrate that was taken up, while CB_{net} focuses on the C retention within the whole soil system. The assumption of a complete rapid utilization of the added substrate is not applicable to our incubations, in which considerable amounts of cellulose remained in the soil by the end of the incubation after 64 days and considerable priming of SOM was observed. Under such circumstances, which may be more reflective of litter inputs in natural soils, CB_{net} and EUE_{net} differ from the estimated CUE (Fig. 6) both conceptually and numerically, as evidenced by measured biomass increases (Fig. 2) and CUE_L, especially early during the incubation and the exponential growth phase. Thus, CB_{net} and EUE_{net} can be taken to reflect the temporal evolution of the net carbon and energy remaining in the soil after substrate addition. From this perspective, our results indicate a net accumulation of carbon (and energy) in the soil after 32 days, as the combined CO_2 (heat) losses from both added cellulose and native SOM do not exceed the amount of initially added carbon (energy) within the time span of the experiment (i.e., CB_{net}, $EUE_{net} > 0$). While the interpretation of these value is thus more akin to a storage efficiency (Manzoni et al., 2018), they themselves do not reveal the nature of the carbon (energy) remaining in the soil, e.g., as undecomposed cellulose, biomass, or necromass.

A more complex understanding of the connection between CR and CUE beyond the simple correspondence suggested by Eqn. (14) can be leveraged to interpret the experimental patterns. This has been demonstrated theoretically for the case of SOM utilization and anaerobic pathways (Chakrawal et al., 2020) as well as using process-based models calibrated to experimental data, which explicitly considered anaerobic and maintenance processes (Endress et al., 2024a). Likewise, the results of our model calibration offer the most nuanced interpretation of the efficiency and carbon-energy coupling over the course of the experiments. First, CB_{net}, EUE_{net} and CUE_L estimated from model output are in good agreement with those obtained from data, although model CUE_L tended to be slightly lower than experimental values due to the inclusion of necromass in the model carbon balance, which is missing from Eqn. (13) (Fig. 6). The model provides a mechanistic description that shows a plausible and consistent interpretation of the observed dynamics of all carbon pools in combination with the total heat production, despite the failure of a simple estimate like CUE_{Rq} in Eqn. (14). In addition, the model offers dynamic estimates of the actual growth efficiencies, i.e., the ratio of (cumulative) biomass formation to the (cumulative) amount of consumed substrate, both for ^{12}C and the combined $^{12}C + {}^{13}C$ pools (Supplementary Fig. S4). These include negative values corresponding to net loss of (^{12}C or total) biomass compared to initial measured values, which is also evident from the experimental biomass time series, and reveal periods of highly efficient growth on SOM, e.g., in the RE-FYM soil (Supplementary Fig. S4). Overall, the model nonetheless suggests that growth was predominantly driven by consumption of the added cellulose in most soils, in particular early during the incubation.

While the use of a labeled substrate is essential for this kind of detailed model calibration and greatly enhances model performance, the calibrated model parameters (e.g., γ_{SOM}) and behavior should still be treated with caution. In particular, models of soil C cycling such as the one employed here frequently face substantial equifinality and limited parameter identifiability (Sierra et al., 2015; Marschmann et al., 2019). Moreover, our model formulation relied on a simple threshold parameter to capture the observed levels of undecomposed cellulose remaining in the soil, and we used a simple conversion of biomass to CO_2 and heat to represent the bioenergetic coupling during maintenance, as opposed to a more complex process like continued SOM use to fuel maintenance requirements. The more detailed characterization of such processes as well as a systematic analysis of model parameter identifiability in the presence of labeled substrates will be critical next steps for the proper representation of microbial-explicit C cycling in biogeochemical models, which remains challenging (Wieder et al., 2015).

4.4. Technical constraints in the combination of C and heat fluxes to dissipate the CR

Although Eqn. (14) from Hansen et al. (2004) shows a relationship between CR and CUE, it is limited to the exponential growth phase fueled by cellulose consumption and is therefore not applicable during maintenance processes or in the case of simultaneous utilization of substrates with different degrees of reduction. As stated by Yang et al. (2024), the accuracy requirements of this model for the CR and the actual determination errors of currently available instruments, such as

TAM Air, imply that CUE can only be inferred from the CR in a best-case scenario. If the heat measurement takes place in low-activity soils at levels close to the detection limit, the stability of the baseline for long-term experiments (e.g. over weeks) can no longer be guaranteed, and it may even be in the negative range (Supplementary Fig. S2). For TH and DI, a subsequent baseline correction had to be carried out in order to obtain realistic heat production rates.

5. Conclusion

Measures of microbial CUE and EUE are frequently based on the fate of added substrates, thus neglecting microbial use of native SOC. We extended these concepts to the net balances of C (CB_{net}) and energy (EUE_{net}) of the whole soil system, which also integrate additional C and energy fluxes due to microbial SOC consumption. They thus quantify whether the system loses or gains C and energy after substrate addition and complement traditional measures of growth efficiency. Application of these concepts to eight cellulose-amended fertilized and unfertilized arable soils demonstrated a net C and energy gain in all soils after 32 days of incubation, despite substantial SOC priming in all soils as indicated by ^{13}C-labeling. The calorespirometric ratio proved to be a useful metric to link the C and energy fluxes in the presence of priming, showing that the initial energy limitation of microbial growth fueled by cellulose was alleviated by SOC consumption during later stages of incubation. Dynamic modeling further suggested a close connection between microbial SOC utilization and the average energy content of SOC in the studied soils. The applied approaches are well suited for the joint evaluation of C and energy fluxes in soils with high microbial biomass and SOC content, but face some limitations in soils with low microbial activity, highlighting a need for further methodological development. Overall, we demonstrated how a combination of experimental and modeling techniques can disentangle the complex dynamics of microbial substrate and SOC utilization from a bioenergetic perspective.

CRediT authorship contribution statement

Johannes Wirsching: Writing – original draft, Validation, Methodology, Investigation, Formal analysis. **Martin-Georg Endress:** Writing – original draft, Methodology, Formal analysis. **Eliana Di Lodovico:** Writing – review & editing, Investigation. **Sergey Blagodatsky:** Writing – review & editing, Validation. **Christian Fricke:** Writing – review & editing, Validation. **Marcel Lorenz:** Writing – review & editing, Investigation. **Sven Marhan:** Writing – review & editing, Conceptualization. **Ellen Kandeler:** Writing – review & editing, Conceptualization. **Christian Poll:** Writing – review & editing, Supervision, Conceptualization.

Funding

This study was performed within the framework of the German Science Foundation (DFG) Priority Program "SPP 2223 – System ecology of soils – Energy Discharge Modulated by Microbiome and Boundary Conditions (SoilSystems)". The work was funded by the DFG under the grants 465124939, 465120774 and 465120347.

Declaration of competing interest

The authors declare the following financial interests/personal relationships which may be considered as potential competing interests: Christian Poll reports financial support was provided by German Research Foundation. If there are other authors, they declare that they have no known competing financial interests or personal relationships that could have appeared to influence the work reported in this paper.

Acknowledgements

The authors acknowledge support by the State of Baden-Württemberg through bwHPC. We would like to thank Wolfgang Armbruster from Institute for Food Chemistry in Hohenheim for the IRMS analysis. Fig. 1 was created using BioRender.

Appendix A. Supplementary data

Supplementary data to this article can be found online at https://doi.org/10.1016/j.soilbio.2024.109691.

References

Ahrends, H.E., Eugster, W., Gaiser, T., Rueda-Ayala, V., Hüging, H., Ewert, F., Siebert, S., 2018. Genetic yield gains of winter wheat in Germany over more than 100 years (1895–2007) under contrasting fertilizer applications. Environmental Research Letters 13, 104003. https://doi.org/10.1088/1748-9326/aade12.

Arcand, M.M., Levy-Booth, D.J., Helgason, B.L., 2017. Resource legacies of organic and conventional management differentiate soil microbial carbon use. Frontiers in Microbiology 8, 309266. https://doi.org/10.3389/fmicb.2017.02293.

Assael, M.J., Maitland, G.C., Maskow, T., von Stockar, U., Wakeham, W.A., Will, S., 2022. Commonly Asked Questions in Thermodynamics. CRC Press.

Barros, N., 2021. Thermodynamics of soil microbial metabolism: applications and functions. Applied Sciences 11, 4962. https://doi.org/10.3390/app11114962.

Barros, N., Feijóo, S., Simoni, A., Critter, S., Airoldi, C., 2000. Interpretation of the metabolic enthalpy change, δhmet, calculated for microbial growth reactions in soils. Journal of Thermal Analysis and Calorimetry 63, 577–588. https://doi.org/10.1023/A:1010162425574.

Barros, N., Hansen, L., Piñeiro, V., Pérez-Cruzado, C., Villanueva, M., Proupín, J., Rodríguez-Añón, J., 2016. Factors influencing the calorespirometric ratios of soil microbial metabolism. Soil Biology and Biochemistry 92, 221–229. https://doi.org/10.1016/j.soilbio.2015.10.007.

Bates, D., Mächler, M., Bolker, B., Walker, S., 2008. Fitting linear mixed-effects models using the lme4 package in r. In: Presentation at Potsdam GLMM Workshop.

Blagodatskaya, E., Khomyakov, N., Myachina, O., Bogomolova, I., Blagodatsky, S., Kuzyakov, Y., 2014. Microbial interactions affect sources of priming induced by cellulose. Soil Biology and Biochemistry 74, 39–49. https://doi.org/10.1016/j.soilbio.2014.02.017.

Blagodatsky, S., Richter, O., 1998. Microbial growth in soil and nitrogen turnover: a theoretical model considering the activity state of microorganisms. Soil Biology and Biochemistry 30, 1743–1755. https://doi.org/10.1016/S0038-0717(98)00028-5.

Boos, E.F., Bruun, S., Magid, J., 2023. Priming is frequently overestimated in studies using ^{14}C-labelled substrates due to underestimation of $^{14}CO_2$ activity. Soil Biology and Biochemistry 181, 109020. https://doi.org/10.1016/j.soilbio.2023.109020.

Bölscher, T., Vogel, C., Olagoke, F.K., Meurer, K.H., Herrmann, A.M., Colombi, T., Brunn, M., Domeignoz-Horta, L.A., 2024. Beyond growth: the significance of non-growth anabolism for microbial carbon-use efficiency in the light of soil carbon stabilisation. Soil Biology and Biochemistry 193, 109400. https://doi.org/10.1016/j.soilbio.2024.109400.

Cagnarini, C., Lofts, S., D'Acqui, L.P., Mayer, J., Grüter, R., Tandy, S., Schulin, R., Costerousse, B., Orlandini, S., Renella, G., 2021. Modelling of long-term zn, cu, cd and pb dynamics from soils fertilised with organic amendments. Soils 7, 107–123. https://doi.org/10.5194/soil-7-107-2021.

Calabrese, S., Chakrawal, A., Manzoni, S., Van Cappellen, P., 2021. Energetic scaling in microbial growth. Proceedings of the National Academy of Sciences 118, e2107668118. https://doi.org/10.1073/pnas.2107668118.

Chakrawal, A., Herrmann, A., Šantrková, H., Manzoni, S., 2020. Quantifying microbial metabolism in soils using calorespirometry—a bioenergetics perspective. Soil Biology and Biochemistry 148, 107945. https://doi.org/10.1016/j.soilbio.2020.107945.

Chakrawal, A., Herrmann, A.M., Manzoni, S., 2021. Leveraging energy flows to quantify microbial traits in soils. Soil Biology and Biochemistry 155, 108169. https://doi.org/10.1016/j.soilbio.2021.108169.

Datta, R., Kelkar, A., Baraniya, D., Molaei, A., Moulick, A., Meena, R.S., Formanek, P., 2017. Enzymatic degradation of lignin in soil: a review. Sustainability 9, 1163. https://doi.org/10.3390/su9071163.

De Graaff, M.A., Classen, A.T., Castro, H.F., Schadt, C.W., 2010. Labile soil carbon inputs mediate the soil microbial community composition and plant residue decomposition rates. New Phytologist 188, 1055–1064. https://doi.org/10.1111/j.1469-8137.2010.03427.x.

Domeignoz-Horta, L.A., Pold, G., Liu, X.J.A., Frey, S.D., Melillo, J.M., DeAngelis, K.M., 2020. Microbial diversity drives carbon use efficiency in a model soil. Nature Communications 11, 3684. https://doi.org/10.1038/s41467-020-17502-z.

Ellmer, F., Baumecker, M., 2005. Static nutrient depletion experiment thyrow. results after 65 experimental years. Archives of Agronomy and Soil Science 51, 151–161. https://doi.org/10.1080/03650340400026669.

Endress, M.G., Chen, R., Blagodatskaya, E., Blagodatsky, S., 2024a. The coupling of carbon and energy fluxes reveals anaerobiosis in an aerobic soil incubation with a Bacillota-dominated community. Soil Biology and Biochemistry 195, 109478. https://doi.org/10.1016/j.soilbio.2024.109478.

Endress, M.G., Dehghani, F., Blagodatsky, S., Reitz, T., Schlüter, S., Blagodatskaya, E., 2024b. Spatial substrate heterogeneity limits microbial growth as revealed by the joint experimental quantification and modeling of carbon and heat fluxes. Soil Biology and Biochemistry 197. https://doi.org/10.1016/j.soilbio.2024.109509.
Fernández, J.M., Plante, A.F., Leifeld, J., Rasmussen, C., 2011. Methodological considerations for using thermal analysis in the characterization of soil organic matter. Journal of Thermal Analysis and Calorimetry 104, 389–398. https://doi.org/10.1007/s10973-010-1145-6.
Fontaine, S., Mariotti, A., Abbadie, L., 2003. The priming effect of organic matter: a question of microbial competition? Soil Biology and Biochemistry 35, 837–843. https://doi.org/10.1016/S0038-0717(03)00123-8.
Geyer, K.M., Dijkstra, P., Sinsabaugh, R., Frey, S.D., 2019. Clarifying the interpretation of carbon use efficiency in soil through methods comparison. Soil Biology and Biochemistry 128, 79–88. https://doi.org/10.1016/j.soilbio.2018.09.036.
Geyer, K.M., Kyker-Snowman, E., Grandy, A.S., Frey, S.D., 2016. Microbial carbon use efficiency: accounting for population, community, and ecosystem-scale controls over the fate of metabolized organic matter. Biogeochemistry 127, 173–188. https://doi.org/10.1007/s10533-016-0191-y.
Gommers, P., Van Schie, B., Van Dijken, J., Kuenen, J., 1988. Biochemical limits to microbial growth yields: an analysis of mixed substrate utilization. Biotechnology and Bioengineering 32, 86–94. https://doi.org/10.1002/bit.260320112.
Hagerty, S.B., Allison, S.D., Schimel, J.P., 2018. Evaluating soil microbial carbon use efficiency explicitly as a function of cellular processes: implications for measurements and models. Biogeochemistry 140, 269–283. https://doi.org/10.1007/s10533-018-0489-z.
Hansen, L.D., Macfarlane, C., McKinnon, N., Smith, B.N., Criddle, R.S., 2004. Use of calorespirometric ratios, heat per CO_2 and heat per O_2, to quantify metabolic paths and energetics of growing cells. Thermochimica Acta 422, 55–61. https://doi.org/10.1016/j.tca.2004.05.033.
Herrmann, A.M., Bölscher, T., 2015. Simultaneous screening of microbial energetics and CO_2 respiration in soil samples from different ecosystems. Soil Biology and Biochemistry 83, 88–92. https://doi.org/10.1016/j.soilbio.2015.01.020.
Ingraham, J.L., Maaløe, O., Neidhardt, F.C., et al., 1983. Growth of the Bacterial Cell. Sinauer Associates Sunderland, MA.
Kästner, M., Maskow, T., Miltner, A., Lorenz, M., Thiele-Bruhn, S., 2024. Assessing energy fluxes and carbon use in soil as controlled by microbial activity-a thermodynamic perspective a perspective paper. Soil Biology and Biochemistry 193, 109403. https://doi.org/10.1016/j.soilbio.2024.109403.
Keiluweit, M., Nico, P.S., Kleber, M., Fendorf, S., 2016. Are oxygen limitations under recognized regulators of organic carbon turnover in upland soils? Biogeochemistry 127, 157–171. https://doi.org/10.1007/s10533-015-0180-6.
Kemp, R., 2000. "fire burn and cauldron bubble"(w. shakespeare): what the calorimetric–respirometric (cr) ratio does for our understanding of cells? Thermochimica Acta 355, 115–124. https://doi.org/10.1016/S0040-6031(00)00442-1.
Klemm, D., Heublein, B., Fink, H.P., Bohn, A., 2005. Cellulose: fascinating biopolymer and sustainable raw material. Angewandte Chemie International Edition 44, 3358–3393. https://doi.org/10.1002/anie.200460587.
Kroschewski, B., Richter, C., Baumecker, M., Kautz, T., 2023. Effect of crop rotation and straw application in combination with mineral nitrogen fertilization on soil carbon sequestration in the thyrow long-term experiment thy_d5. Plant and Soil 488, 121–136. https://doi.org/10.1007/s11104-022-05459-5.
Lacroix, E.M., Mendillo, J., Gomes, A., Dekas, A., Fendorf, S., 2022. Contributions of anoxic microsites to soil carbon protection across soil textures. Geoderma 425, 116050. https://doi.org/10.1016/j.geoderma.2022.116050.
Lorenz, M., Blagodatskaya, E., Finn, D., Fricke, C., Hüging, H., Kandeler, E., Kaiser, K., Kästner, M., Lechtenfeld, O., Marhan, S., Maskow, T., Mayer, J., Miltner, A., Normant-Saremba, M., Poll, C., Resseguier, C., Rupp, A., Schrumpf, M., Schweitzer, K., Simon, C., Tebbe, C., Yang, S., Yousaf, U., Thiele-Bruhn, S., 2024a. Database for the Priority Program 2322 SoilSystems – Soils and Substrates Used in the First Phase (2021-2024). https://doi.org/10.5281/zenodo.11207502.
Lorenz, M., Maskow, T., Thiele-Bruhn, S., 2024b. Energy stored in soil organic matter is influenced by litter quality and the degree of transformation–a combustion calorimetry study. Geoderma 443, 116846. https://doi.org/10.1016/j.geoderma.2024.116846.
Manzoni, S., Čapek, P., Porada, P., Thurner, M., Winterdahl, M., Beer, C., Brüchert, V., Frouz, J., Herrmann, A.M., Lindahl, B.D., et al., 2018. Reviews and syntheses: carbon use efficiency from organisms to ecosystems–definitions, theories, and empirical evidence. Biogeosciences 15, 5929–5949. https://doi.org/10.5194/bg-15-5929-2018.
Manzoni, S., Taylor, P., Richter, A., Porporato, A., Ågren, G.I., 2012. Environmental and stoichiometric controls on microbial carbon-use efficiency in soils. New Phytologist 196, 79–91. https://doi.org/10.1111/j.1469-8137.2012.04225.x.
Marschmann, G.L., Pagel, H., Kügler, P., Streck, T., 2019. Equifinality, sloppiness, and emergent structures of mechanistic soil biogeochemical models. Environmental Modelling & Software 122, 104518. https://doi.org/10.1016/j.envsoft.2019.104518.
Nest, T.V., Ruysschaert, G., Vandecasteele, B., Houot, S., Baken, S., Smolders, E., Cougnon, M., Reheul, D., Merckx, R., 2016. The long term use of farmyard manure and compost: effects on p availability, orthophosphate sorption strength and p leaching. Agriculture, Ecosystems & Environment 216, 23–33. https://doi.org/10.1016/j.agee.2015.09.009.
Newville, M., Otten, R., Nelson, A., Stensitzki, T., Ingargiola, A., Allan, D., Fox, A., Carter, F., Michał, Osborn, R., Pustakhod, D., lneuhaus, Weigand, S., Aristov, A., Glenn, Deil, C., mgunyho, Mark, Hansen, A.L.R., Pasquevich, G., Foks, L., Zobrist, N., Frost, O., Stuermer, azelcer, Polloreno, A., Persaud, A., Nielsen, J.H., Pompili, M., Eendebak, P., 2023. Lmfit/Lmfit-Py: 1.2.2. https://doi.org/10.5281/zenodo.8145703.
Öquist, M.G., Erhagen, B., Haei, M., Sparrman, T., Ilstedt, U., Schleucher, J., Nilsson, M. B., 2017. The effect of temperature and substrate quality on the carbon use efficiency of saprotrophic decomposition. Plant and Soil 414, 113–125. https://doi.org/10.1007/s11104-016-3104-x.
Panikov, N., 1996. Mechanistic mathematical models of microbial growth in bioreactors and in natural soils: explanation of complex phenomena. Mathematics and Computers in Simulation 42, 179–186. https://doi.org/10.1016/0378-4754(95)00127-1.
Perveen, N., Barot, S., Maire, V., Cotrufo, M.F., Shahzad, T., Blagodatskaya, E., Stewart, C.E., Ding, W., Siddiq, M.R., Dimassi, B., et al., 2019. Universality of priming effect: an analysis using thirty five soils with contrasted properties sampled from five continents. Soil Biology and Biochemistry 134, 162–171. https://doi.org/10.1016/j.soilbio.2019.03.027.
Piepho, H., Büchse, A., Richter, C., 2004. A mixed modelling approach for randomized experiments with repeated measures. Journal of Agronomy and Crop Science 190, 230–247. https://doi.org/10.1111/j.1439-037X.2004.00097.x.
Poll, C., Pagel, H., Devers-Lamrani, M., Martin-Laurent, F., Ingwersen, J., Streck, T., Kandeler, E., 2010. Regulation of bacterial and fungal mcpa degradation at the soil–litter interface. Soil Biology and Biochemistry 42, 1879–1887. https://doi.org/10.1016/j.soilbio.2010.07.013.
Popovic, M., Woodfield, B.F., Hansen, L.D., 2019. Thermodynamics of hydrolysis of cellulose to glucose from 0 to 100°c: cellulosic biofuel applications and climate change implications. The Journal of Chemical Thermodynamics 128, 244–250. https://doi.org/10.1016/j.jct.2018.08.006.
Qiao, Y., Wang, J., Liang, G., Du, Z., Zhou, J., Zhu, C., Huang, K., Zhou, X., Luo, Y., Yan, L., et al., 2019. Global variation of soil microbial carbon-use efficiency in relation to growth temperature and substrate supply. Scientific Reports 9, 5621. https://doi.org/10.1038/s41598-019-42145-6.
Saito, T., Kimura, S., Nishiyama, Y., Isogai, A., 2007. Cellulose nanofibers prepared by tempo-mediated oxidation of native cellulose. Biomacromolecules 8, 2485–2491. https://doi.org/10.1021/bm0703970.
Sierra, C.A., Malghani, S., Müller, M., 2015. Model structure and parameter identification of soil organic matter models. Soil Biology and Biochemistry 90, 197–203. https://doi.org/10.1016/j.soilbio.2015.08.012.
Sørensen, T.H., Cruys-Bagger, N., Borch, K., Westh, P., 2015. Free energy diagram for the heterogeneous enzymatic hydrolysis of glycosidic bonds in cellulose. Journal of Biological Chemistry 290, 22203–22211. https://doi.org/10.1074/jbc.M115.659656.
Vance, E.D., Brookes, P.C., Jenkinson, D.S., 1987. An extraction method for measuring soil microbial biomass C. Soil Biology and Biochemistry 19, 703–707. https://doi.org/10.1016/0038-0717(87)90052-6.
Virtanen, P., Gommers, R., Oliphant, T.E., Haberland, M., Reddy, T., Cournapeau, D., Burovski, E., Peterson, P., Weckesser, W., Bright, J., van der Walt, S.J., Brett, M., Wilson, J., Millman, K.J., Mayorov, N., Nelson, A.R.J., Jones, E., Kern, R., Larson, E., Carey, C.J., Polat, I., Feng, Y., Moore, E.W., VanderPlas, J., Laxalde, D., Perktold, J., Cimrman, R., Henriksen, I., Quintero, E.A., Harris, C.R., Archibald, A.M., Ribeiro, A. H., Pedregosa, F., van Mulbregt, P., SciPy 1.0 Contributors, 2020. SciPy 1.0: fundamental algorithms for scientific computing in Python. Nature Methods 17, 261–272. https://doi.org/10.1038/s41592-019-0686-2.
Von Stockar, U., Liu, J.S., 1999. Does microbial life always feed on negative entropy? thermodynamic analysis of microbial growth. Biochimica et Biophysica Acta (BBA) - Bioenergetics 1412, 191–211. https://doi.org/10.1016/S0005-2728(99)00065-1.
Von Stockar, U., Maskow, T., Liu, J., Marison, I.W., Patino, R., 2006. Thermodynamics of microbial growth and metabolism: an analysis of the current situation. Journal of Biotechnology 121, 517–533. https://doi.org/10.1016/j.jbiotec.2005.08.012.
Wang, C., Kuzyakov, Y., 2023. Energy use efficiency of soil microorganisms: driven by carbon recycling and reduction. Global Change Biology 29, 6170–6187. https://doi.org/10.1111/gcb.16925.
Wieder, W.R., Allison, S.D., Davidson, E.A., Georgiou, K., Hararuk, O., He, Y., Hopkins, F., Luo, Y., Smith, M.J., Sulman, B., Todd-Brown, K., Wang, Y., Xia, J., Xu, X., 2015. Explicitly representing soil microbial processes in earth system models. Global Biogeochemical Cycles 29, 1782–1800. https://doi.org/10.1002/2015GB005188.
Yang, S., Di Lodovico, E., Rupp, A., Harms, H., Fricke, C., Miltner, A., Kaestner, M., Maskow, T., 2024. Enhancing insights: exploring the information content of calorespirometric ratio in dynamic soil microbial growth processes through calorimetry. Frontiers in Microbiology 15, 1321059. https://doi.org/10.3389/fmicb.2024.1321059.